Hindawi Publishing Corporation
Shock and Vibration
Volume 2016, Article ID 3109385, 14 pages
http://dx.doi.org/10.1155/2016/3109385

Research Article

Partly Duffing Oscillator Stochastic Resonance Method and Its Application on Mechanical Fault Diagnosis

Jian Dang,[1,2] Rong Jia,[1,2] Xingqi Luo,[1,2] Hua Wu,[2] and Diyi Chen[3]

[1]*State Key Laboratory Base of Eco-Hydraulic Engineering in Arid Area, Xi'an University of Technology, Xi'an 710048, China*
[2]*Institute of Water Resources and Hydro-Electric Engineering, Xi'an University of Technology, Xi'an 710048, China*
[3]*Institute of Water Resources and Hydropower Research, Northwest A&F University, Yangling 712100, China*

Correspondence should be addressed to Rong Jia; jiarong@xaut.edu.cn

Received 4 July 2016; Revised 12 September 2016; Accepted 24 October 2016

Academic Editor: Pedro Galvín

Due to the fact that the slight fault signals in early failure of mechanical system are usually submerged in heavy background noise, it is unfeasible to extract the weak fault feature via the traditional vibration analysis. Stochastic resonance (SR), as a method of utilizing noise to amplify weak signals in nonlinear dynamical systems, can detect weak signals overwhelmed in the noise. However, based on the analysis of the impact of noise intensity on SR effect, it is concluded that the detection results are dramatically limited by the noise intensity of measured signals, especially for incipient fault feature of mechanical system with poor working environment. Therefore, this paper proposes a partly Duffing oscillator SR method to extract the fault feature of mechanical system. In this method, to locate the appearance of weak fault feature and decrease noise intensity, the permutation entropy index is constructed to select the measured signals for the input of Duffing oscillator system. Then, according to the regulation of system parameters, a reasonable match between the selected signals and Duffing oscillator model is achieved to produce a SR phenomenon and realize the fault diagnosis of mechanical system. Experiment results demonstrate that the proposed method achieves a better effect on the fault diagnosis of mechanical system.

1. Introduction

With the rapid development of science and technology, rotating machinery plays a significant role in a wide range of industrial applications, such as the hydroelectric turbine, wind turbines, aeroengine, transportation vehicles, and machine tools. Hence, it is of great significance to research fault diagnosis methods of incipient fault prognoses and guaranteeing the reliability of the mechanical system [1]. In the past decades, many algorithms are proposed in the area of mechanical fault diagnosis [2–6]. However, as researchers found, the rotating machine is a complicated and nonlinear system, and it has been proven that the incipient fault feature is usually overwhelmed in heavy background noise from other coupled machine components and measuring instruments, which makes it difficult to detect the weak feature signal clearly.

In 1981, stochastic resonance (SR) was firstly introduced by Benzi et al. [7] and C. Nicolis and G. Nicolis [8] in their study on explaining the periodic recurrences of the earth's ice ages. As a nonlinear signal processing method, the output signals of system can be enhanced with optimized signal-to-noise ratios (SNR) with the assistance of proper intensity noise. Therefore, substantive researches have been done on SR in the area of weak signal detection [9–15]. In the past few years, in order to improve the output effect of traditional one-dimensional Langevin system, Gammaitoni et al. first introduced SR for the two-dimensional bistable Duffing oscillator system [16, 17], and then the related simulation analysis and experimental research on the output characteristics were discussed [18, 19]. On this basis, Leng et al. [20, 21] proposed that, with the introduction of tunable damping ratio in the Duffing oscillator model, it is possible to realize SR for signals with different noise intensity.

However, based on the previous research, the impact of noise intensity on SR effect is discussed and it is found that the output effect has a significant decrease with the increase of noise intensity even though the optimal system

Table 1: Average of permutation entropy of test signal under various SNR.

SNR	Waveform	Permutation entropy (AVG)
Base signal	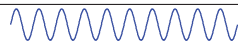	0.052
20 dB		0.527
10 dB		0.656
0 dB		0.795
White noise		0.988

parameters have been achieved. Thus, it can be concluded that the signal detection result is dramatically limited by the noise intensity of measured signals in Duffing oscillator SR, especially for incipient fault feature of mechanical system with poor working environment and strong noise background. Therefore, a partly Duffing oscillator SR method based on permutation entropy is proposed in this paper. Permutation entropy, as a statistical measurement method, has high sensibility to abrupt dynamic change [22, 23]; thus it can serve as an index to detect slight signal change and locate the appearance of fault feature. Based on variation curves of permutation entropy, the original signals are selected to decrease the signal size and noise intensity, which overcomes the shortcoming of the detecting results limited by noise intensity in traditional SR methods. Then, according to the regulation of system parameters, a reasonable match between the selected signals and Duffing oscillator model is achieved to produce a SR phenomenon and realize the fault feature extraction. Experiment results demonstrate that the proposed method achieves a better effect on the fault diagnosis of rotating machinery.

This paper is organized as follows. The theory of Duffing oscillator SR and influence of noise intensity on SR effect is introduced in Section 2. Section 3 describes the algorithm of permutation entropy which is introduced in the partly Duffing oscillator SR method. Then, the effectiveness of the proposed method is verified by the engineering application in Section 4. Finally, conclusions are drawn in Section 5.

2. Brief Review of SR

2.1. Theory of Duffing Oscillator SR. Nowadays, most research about traditional SR methods focuses on the Langevin model [24]. However, it has been proven that the SNR of output signal in Duffing oscillator system is higher than that in Langevin system [25]. As shown in Figure 1, the Duffing oscillator is a bistable system with double well potential, which meets the three necessary ingredients for producing a SR phenomenon [7]. The Duffing oscillator system can be described as follows:

$$\ddot{x} + k\dot{x} - ax + bx^3 = s(t) + \sqrt{2D}\xi(t), \quad (1)$$

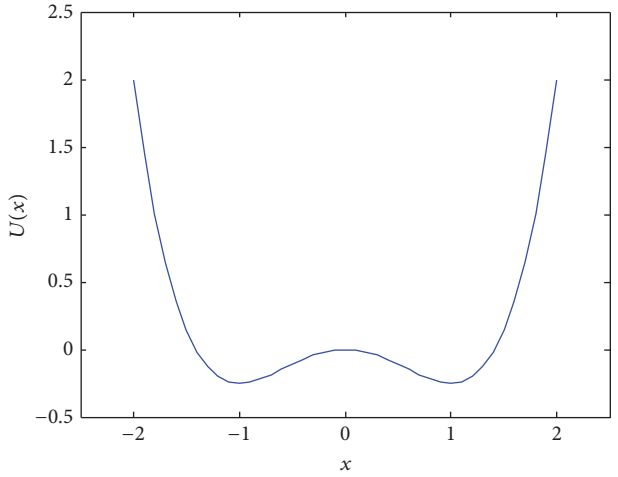

Figure 1: Potential function $U(x)$ of Duffing oscillator system.

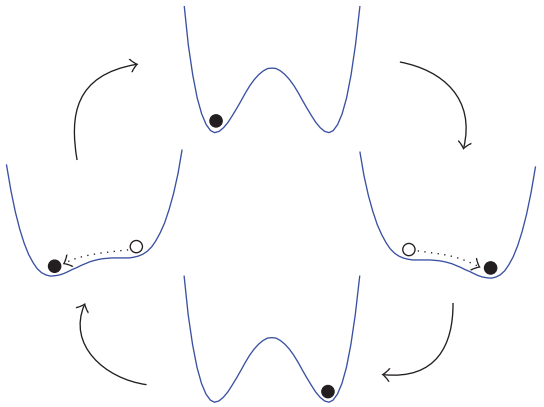

Figure 2: State transition of Duffing oscillator system with the assistance of periodic force and noise.

where the parameters a and b are positive real numbers and the corresponding potential function $U(x) = -ax^2/2 + bx^4/4$, k is the damping ratio and $s(t) = A\sin(2\pi f_0 t)$ is the driving signal, D is the noise intensity, and $\xi(t)$ is a Gaussian white noise. The two separated barriers are formed by two stable fixed points $x_m = \pm\sqrt{a/b}$ and one quasi-stable fixed point at $x_b = 0$ of potential function $U(x)$ in Duffing oscillator system.

With the assistance of proper intensity noise, the Brownian particle will accumulate enough energy to cross the barriers and jump between two potential wells. When the transition rate of Brownian particle matches the signal period, the periodic input signal will be enhanced with SR. Figure 2 displays the state transition of the Duffing oscillator system with the assistance of periodic force and noise.

2.2. The Influence of Noise Intensity on SR Effect. According to the mechanism of Duffing oscillator SR, the weak signal detecting result of SR method is closely related to the noise intensity [21]. In order to analyze the influence of noise intensity on SR effect in Duffing oscillator system, the simulation signals with different noise intensities of $D = 0.5$ and $D = 5$ are constructed, respectively, where the corresponding

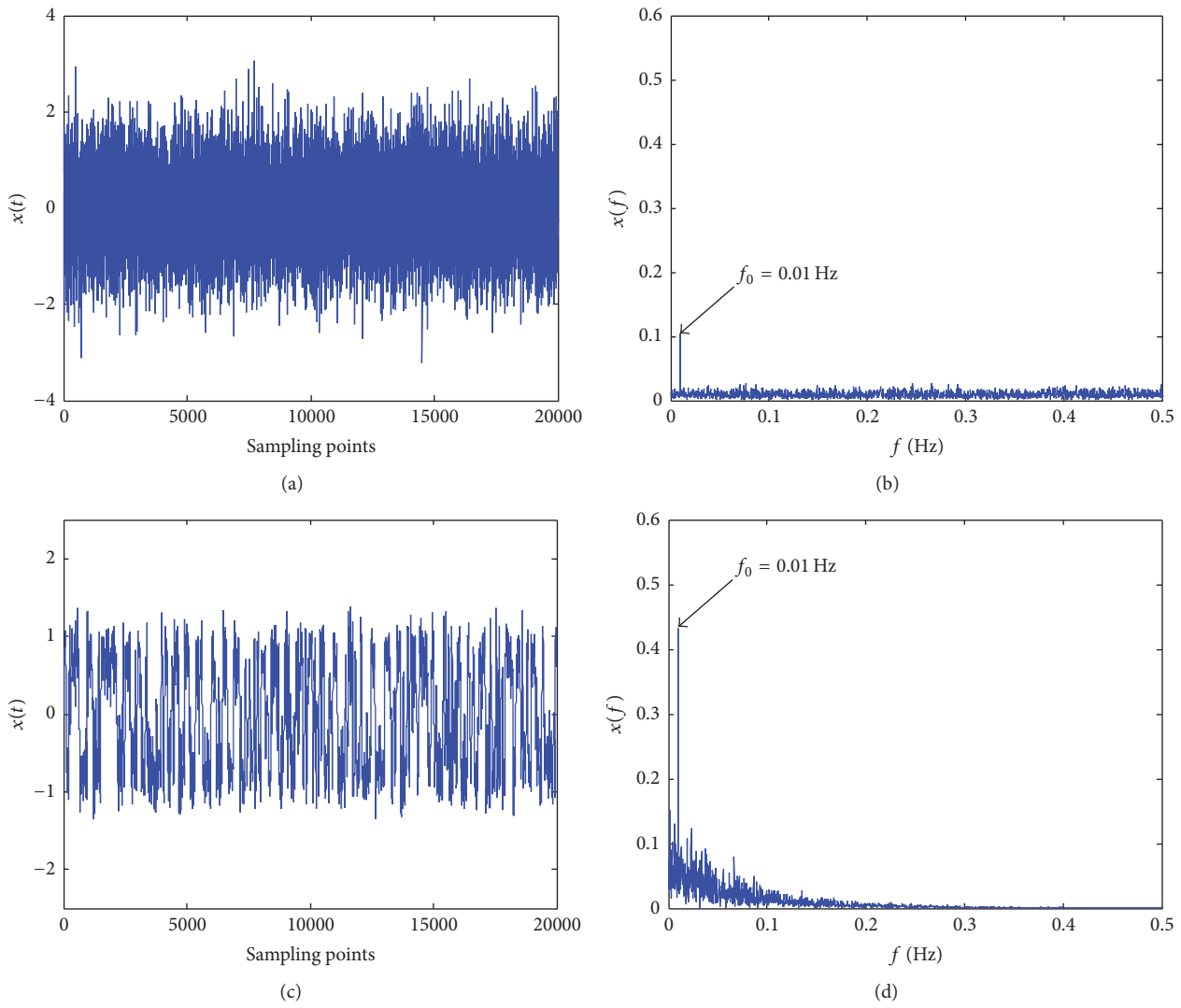

FIGURE 3: Phenomenon of system SR under the noise intensity $D = 0.5$. (a) Time-domain waveform of input signals, (b) frequency spectrum of input signals, (c) time-domain waveform of output signals, and (d) frequency spectrum of output signals.

parameters are set to $A = 0.1$ and $f_0 = 0.01$ Hz. The sample frequency and the system parameters are set at $f_s = 5$ Hz and $a = b = 1$, and damping ratio k is set to $k = 0.5$ and $k = 2.5$, respectively, for producing SR. Figures 3 and 4 show the weak signal detection results of Duffing oscillator SR under different noise intensities. By comparing with the phenomenon in Figure 3, it is apparent that not only does the feature signal amplitude have a significant decrease, but also the frequency spectrum of output signals contains many complex ingredients except the characteristic frequency $f_0 = 0.01$ Hz in Figure 4.

In addition, based on the mechanism analysis of Duffing oscillator SR from the perspective of Kramers rate [26], the condition of realizing the Duffing oscillator SR phenomenon [21] is defined as illustrated in the following equation:

$$F(D, f_0, k, a, b) = \frac{a}{2\sqrt{2}\pi k f_0} \exp\left(-\frac{a^2}{4bD}\right). \quad (2)$$

Apparently, the SR phenomenon is realized when $F = 1$, and it can be seen from (2) that the SR effect is affected by the parameters a and b, the damping ratio k, the signal frequency f_0, and the noise intensity D. Figure 5 displays the change curves of the characteristic signal amplitude Am at $f = f_0$ versus noise intensity D with different parameters a, b, k, and f_0, respectively.

It can be seen from Figure 5 that the characteristic signal amplitude Am first increases and then falls off as noise intensity D increases (observed by the red curves in Figure 5), even if the SR phenomenon has been produced by adjusting the system parameters a, b, and k. What is more, when the noise intensity is relatively large, the characteristic signal amplitude Am has a significant decrease in comparison with that in optimal noise intensity D_{op}. Therefore, it can be inferred that the output signal amplitude Am of traditional SR method is closely related to the noise intensity, and it is difficult to extract the feature signal under a stronger noise

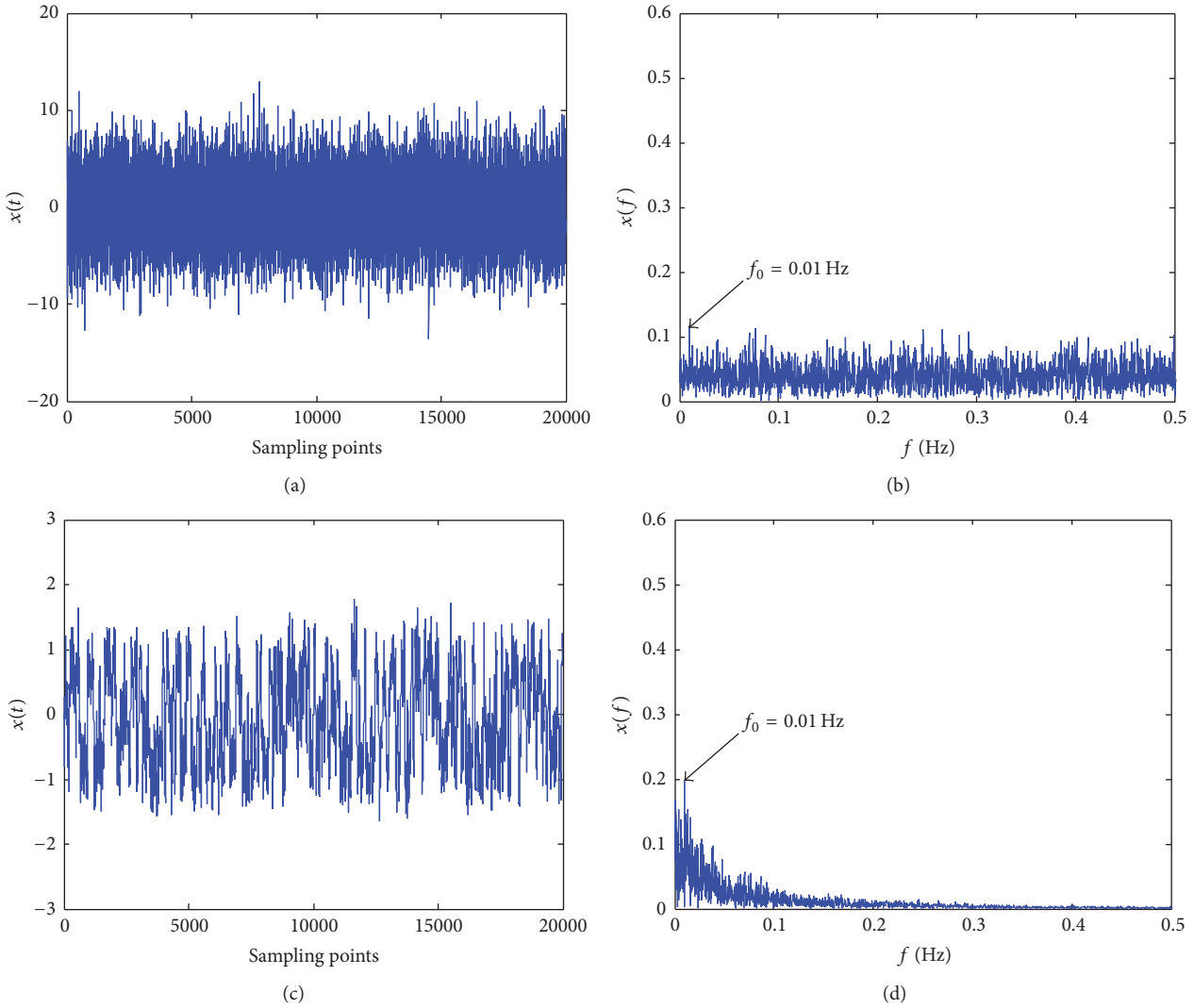

FIGURE 4: Phenomenon of system SR under the noise intensity $D = 5$. (a) Time-domain waveform of input signals, (b) frequency spectrum of input signals, (c) time-domain waveform of output signals, and (d) frequency spectrum of output signals.

background even though the optimal system parameters have been achieved.

3. Partly Duffing Oscillator SR

Based on the previously mentioned conclusion, we are motivated to introduce an index to locate the appearance of slight signals for reducing the noise intensity of the input signals of Duffing oscillator system. Due to the fact that the occurrence of weak feature is usually accompanied by a dynamic change in the measured signals, the similarity measure methods have been presented to detect such changes including Kullback–Leibler divergence [27], l_2-norm [28], and Hausdorff distance [29]. However, most of these methods are based on quantifying the dissimilarity between the reference probability density functions; for the weak signals submerged in the heavy background noise, the dissimilarity is not significant. The complexity measure, in comparison, is computationally more efficient [30], such as Lempel–Ziv complexity [31], approximate entropy [32], and permutation entropy [33], especially for the last one.

As a measure of signal complexity, permutation entropy (PE), which has characteristics of high sensitivity to signal change and simple calculation and strong robustness [34], has been widely applied to research the complexity of the time series and dynamic characteristics [35–38]. Therefore, a partly Duffing oscillator SR method based on PE is proposed in this paper. In this method, to solve the problem of weak signal detection result limited by the noise intensity in traditional SR method, the PE of measured signals is calculated as an index to locate the appearance of weak signals and decrease the noise intensity of the input signals of Duffing oscillator system. Then, according to the regulation of system parameters, a reasonable match between the selected signals and Duffing oscillator model is realized to produce the SR phenomenon for fault diagnosis of rotating machine.

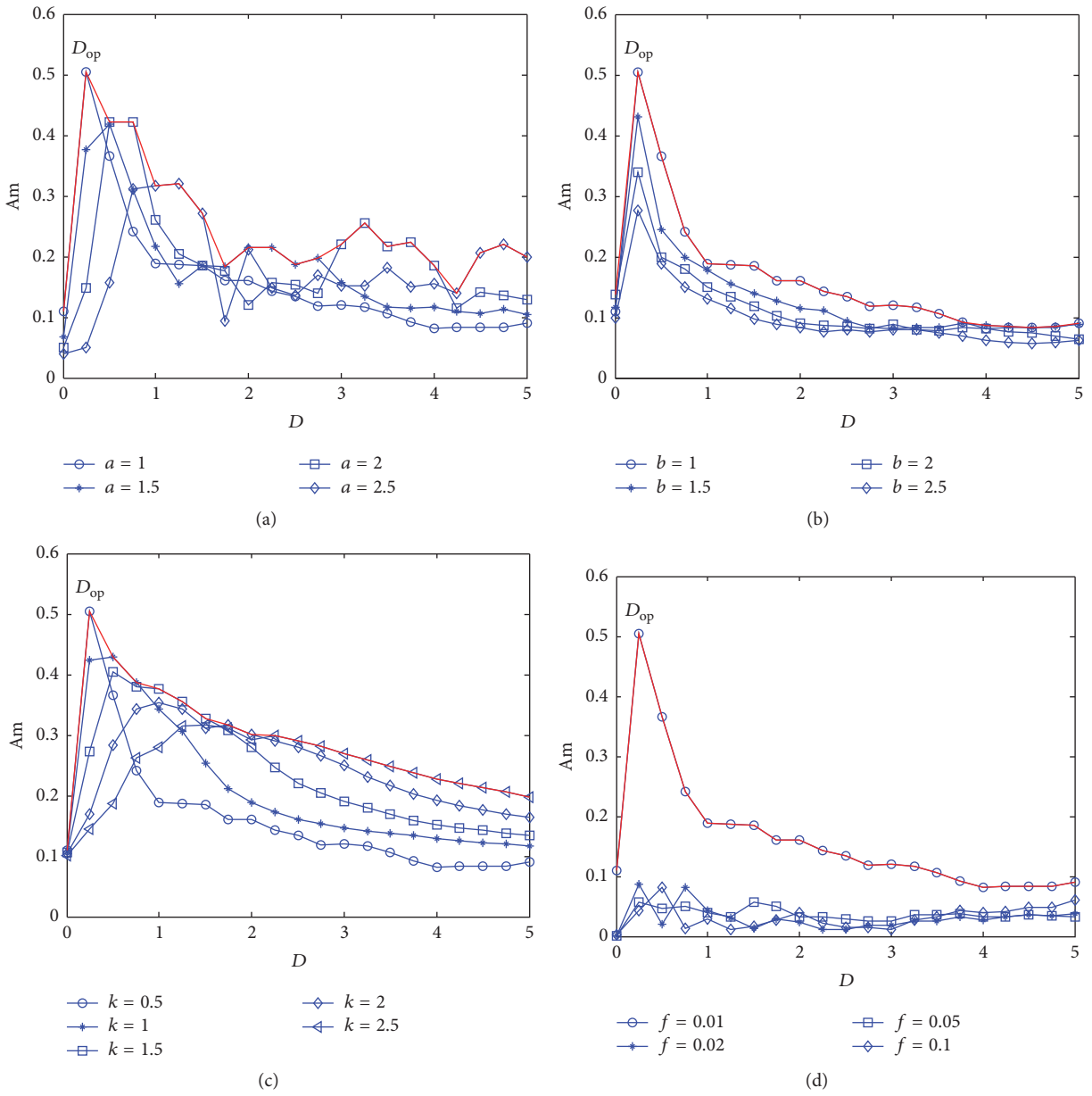

FIGURE 5: The change curves of Duffing oscillator SR effect versus noise intensity D under different conditions. (a) Different parameter a, (b) different parameter b, (c) different damping ratio k, and (d) different signal frequency f.

3.1. Theory of Permutation Entropy. Take the time series $\{x(i), i = 1, 2, \ldots, N\}$ as the example. To analyze the complexity of $x(i)$, the phase space is reconstructed as a higher dimension as follows:

$$X(1) = \{x(1), x(1+\tau), \ldots, x(1+(m-1)\tau)\}$$
$$\vdots$$
$$X(i) = \{x(i), x(i+\tau), \ldots, x(i+(m-1)\tau)\}$$
$$\vdots$$
$$X(N-(m-1)\tau) = \{x(N-(m-1)\tau), x(N-(m-2)\tau), \ldots, x(N)\}, \quad (3)$$

where m and τ represent embedded dimension and time delay, respectively, and each reconstructed vector $X(i)$ can be arranged in an increasing order as described in the following equation:

$$x(i+(j_1-1)\tau) \le x(i+(j_2-1)\tau) \le \cdots \le x(i+(j_m-1)\tau), \quad (4)$$

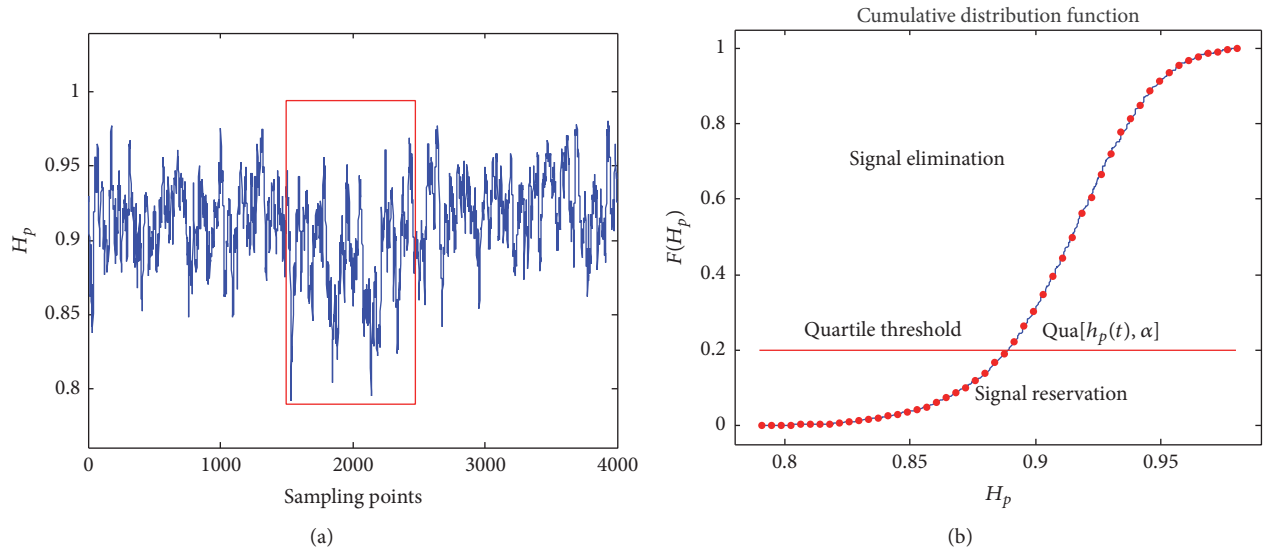

FIGURE 6: The principle of signal selection based on PE. (a) Variation curves of PE values of the simulation signals; (b) the cumulative distribution function of PE values.

where $j_1, j_2, \ldots, j_m$ are the positions of corresponding elements [32]. Therefore, any reconstructed vector $X(i)$ can be mapped onto a group of symbols as follows:

$$S(l) = (j_1, j_2, \ldots, j_m), \tag{5}$$

where $l = 1, 2, \ldots, k$, $k = N-(m-1)\tau$. Owing to the fact that the sequences contain m distinct symbols, the sequences at most have $m!$ types, and $S(l)$ is just one of them. Assume that $P_1, P_2, \ldots, P_k$ can be used to denote the probability distribution of each symbol sequence, respectively; the permutation entropy of order m for $x(i)$ can be defined as the Shannon entropy for the k symbol sequences as

$$H_P(m, \tau) = -\sum_{i=1}^{k} P_i \ln P_i. \tag{6}$$

Then, the PE of order m can be normalized as follows:

$$H_P = \frac{H_P(m, \tau)}{\ln(m!)}. \tag{7}$$

The values of H_P represent the randomness of the time series; the larger the value of H_P, the more random the time series is, and vice versa.

To intuitively observe the validity in reflecting the noise intensity variation of signals, the PE values of sine signals combined with an additive noise are calculated, as listed in Table 1. It can be seen from that that the lower the SNR, the larger the PE values, which means the PE can provide a quantitative tool to reflect the nonlinear change in the measured signals.

3.2. Principle of Signal Selection Based on PE. Motivated by these advantages mentioned above, the PE of the measured signals is constructed in this paper as the index to locate the appearance of weak fault feature. In order to reflect the dynamic change of measured signals in real time, the sliding window is constructed in the measured signals [39], and the permutation entropy $H_P(t)$ is calculated for each data subset. The principle of the signal selection based on PE translates to

$$S(j) = \begin{cases} s(i) & \widehat{H}_P^{(i)}(t) < \text{Qua}\left[h_p(t), \alpha\right] \quad i = 1, 2, 3, \ldots, N \\ 0 & \widehat{H}_P^{(i)}(t) > \text{Qua}\left[h_p(t), \alpha\right] \quad j = 1, 2, 3, \ldots, \end{cases} \tag{8}$$

where $s(i)$ is the original signal and $S(j)$ represents the selected signal for the input of Duffing oscillator system. Qua$[h_p(t), \alpha]$ indicates that the αth quartile of $h_p(t)$ and $\widehat{H}_P^{(i)}(t)$ denotes moving average of $h_p(t)$. In this paper, α is set to 0.8. To clearly illustrate the principle and testify the algorithm's effectiveness, the simulation signals are defined as

$$s(t) = H(t) * \sin(2\pi f_0 * t) + \varepsilon(t), \tag{9}$$

where $H(t)$ is a step function, $H(t) = 0$, and $t \in (0, 150) \cup (250, 400)$; $H(t) = 0.2$; $t \in [150, 250]$. $\varepsilon(t)$ is Gaussian white noise. The characteristic frequency f_0 is 0.1 Hz and the sampling frequency is 10 Hz. The length of data is 4000. Figure 6(a) shows the variation curves of PE values of simulation signals. It can be seen that the PE values have a significant decrease in the case when the regular signal occurs, which indicates that the PE values can be settled as an index to locate the appearance of slight feature signal.

In addition, as illustrated in (8), this paper adopts the quantile based PE thresholding method to the signal selection and the α quantile of PE values is calculated as the threshold. Figure 6(b) depicts the cumulative distribution function (CDF) of PE values of the simulation signals. When the value of PE index is smaller than the set quantile threshold Qua$[h_p(t), \alpha]$, the signal is reversed; otherwise the signal is eliminated. Figures 7 and 8 display the time-domain

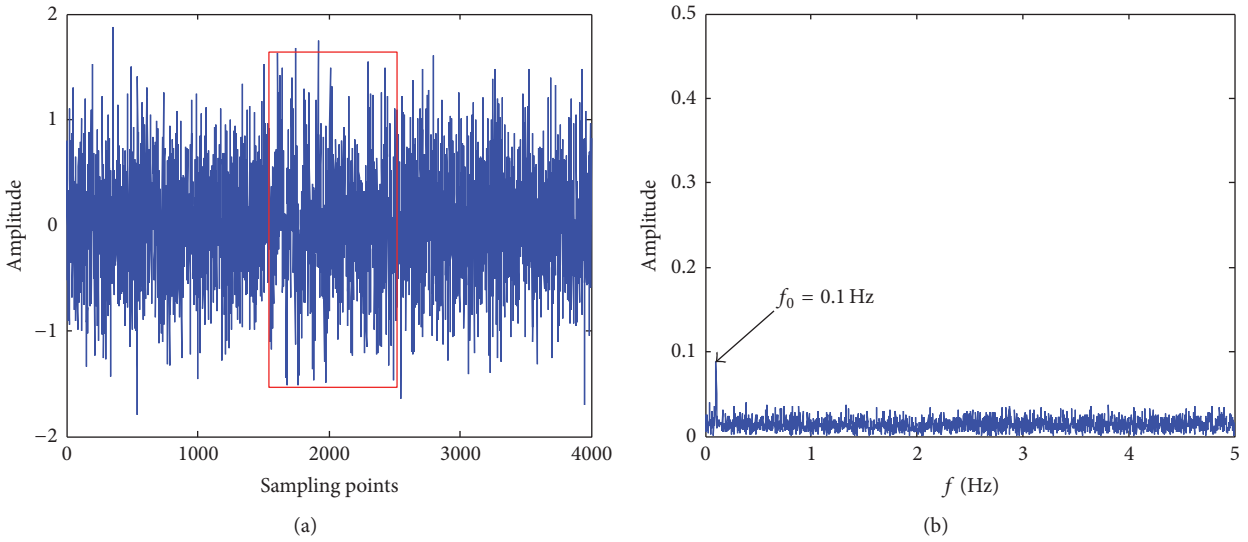

Figure 7: (a) Time-domain waveform of the simulation signals; (b) frequency spectrum of the simulation signals.

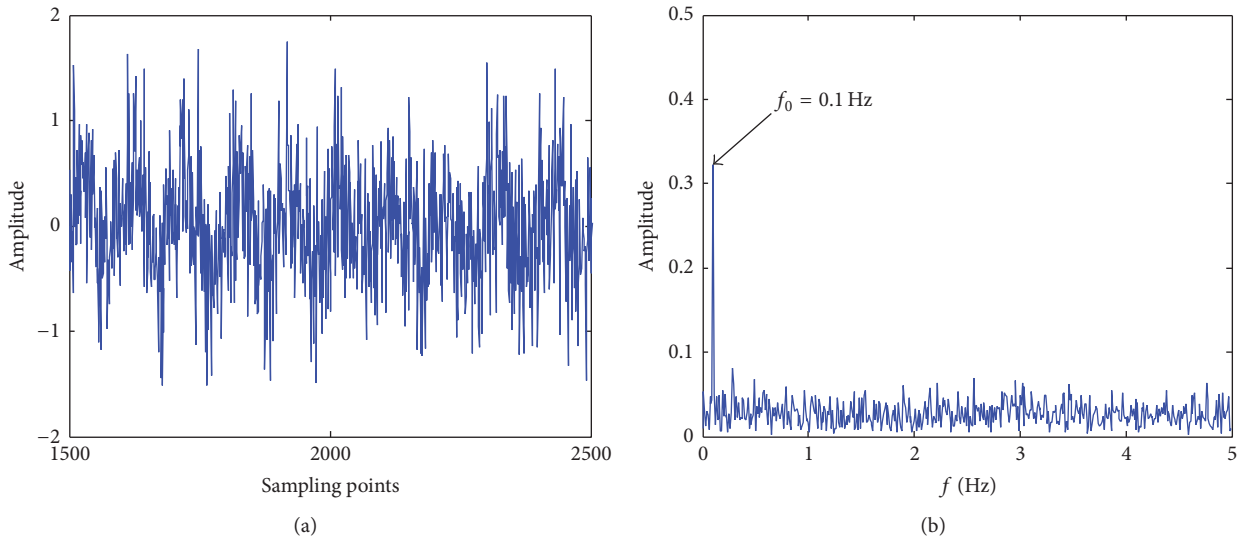

Figure 8: (a) Time-domain waveform of the selected simulation signals; (b) frequency spectrum of the selected simulation signals.

waveforms and frequency spectrum of simulation signals constructed in (9) before and after signal selection by PE index, respectively. By comparison, the algorithm of signal selection based on PE can effectively decrease the signal size and the noise intensity, which is conductive to the weak feature enhancement of Duffing oscillator SR system.

3.3. Procedure of the Proposed Method. The flow chart of the proposed method is shown in Figure 9, with the specific procedure given in the following:

(1) signals.

(2) relevant parameters in proposed method.

(3) Select the signals based on the variation curves of PE:

(3.1) construct variation tendency of PE $h_p(t)$ of measured signals,

(3.2) compute the αth quartile $\mathrm{Qua}[h_p(t), \alpha]$ of the PE values,

(3.3) calculate the moving average $\widehat{H}_P^{(i)}(t)$ of PE. If $\widehat{H}_P^{(i)}(t) < \mathrm{Qua}[h_p(t), \alpha]$, the signal is reserved; $S(j) = s(i)$. Otherwise, the signal is discarded,

(3.4) if i does not reach the sample points N, go to step (3.3) with $i = i + 1$ and $j = j + 1$.

(4) Take the selected signals as the input of Duffing oscillator system.

(5) Based on the regulation of system parameters, a reasonable match between input signals and Duffing

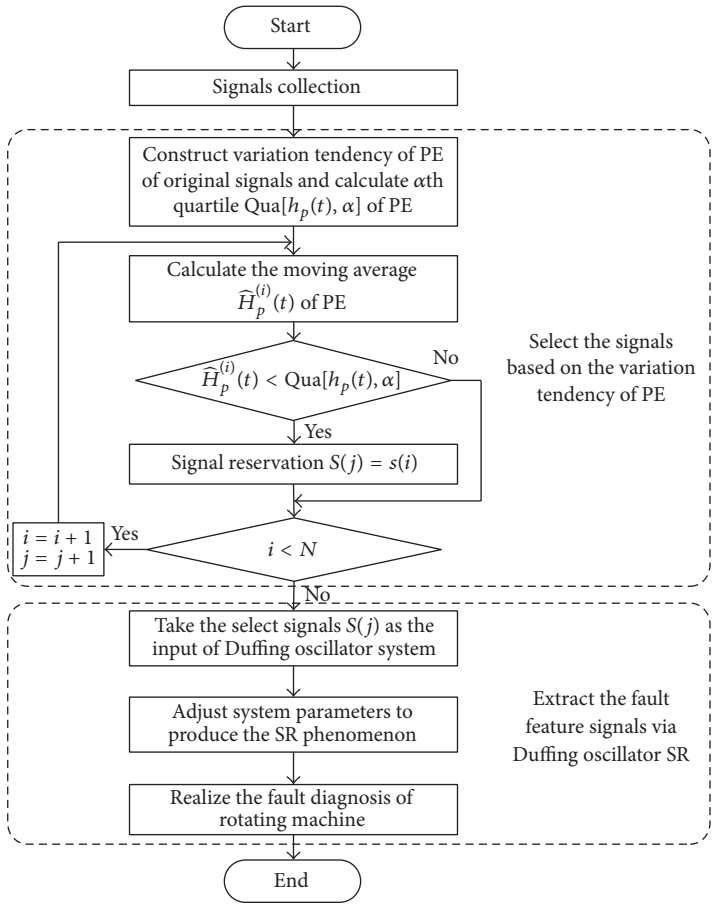

Figure 9: Flow chart of the proposed method.

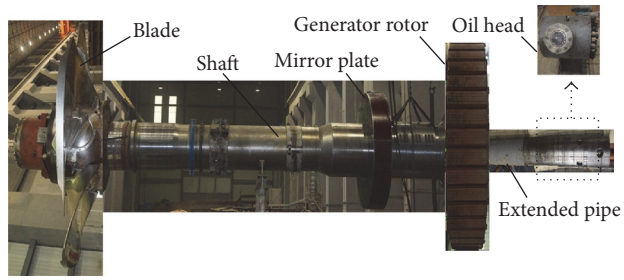

Figure 10: Prototype of hydroelectric turbine.

oscillator model is realized to produce a SR phenomenon.

(6) Realize the fault diagnosis of rotating machine with the utilization of the proposed method.

4. Engineering Application

4.1. Experimental Data Collection. To verify the effectiveness of proposed method in fault diagnosis of rotating machine, the experimental studies on a hydroelectric turbine in upper reaches of Yellow River are conducted. As shown in Figure 10, the experimental signals are acquired from the prototype of hydroelectric turbine with 5 blades, and the rated speed is 107.1 r/min (1.79 Hz). Figure 11 describes specific layout of measuring points of pressure fluctuation signals in the turbine.

In the hydroelectric turbine, due to the fact that the oil supply is generally sustained by the floating tile, the floating tile is usually affected by vibration of the turbine shaft, which makes it prone to wear. In addition, once the floating tile suffers damage, the problems of oil leakage and its diffusion to other channels in the oil supply will lead to the turbine being unfeasible to work in on-cam operating condition. For these reasons, faults on the floating tile in the oil supply are created in the experiment. The pressure fluctuation signals

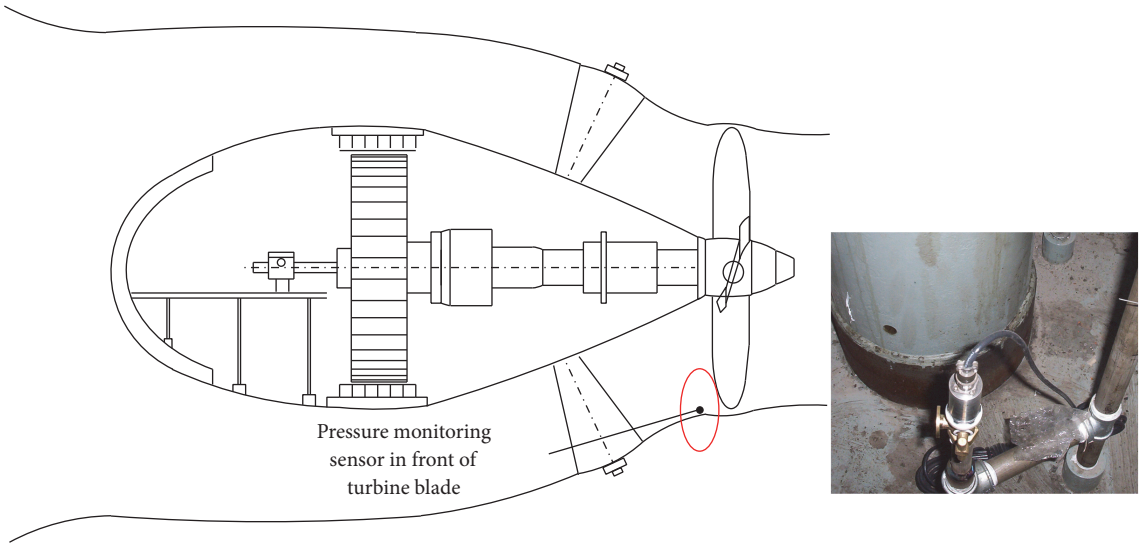

Figure 11: Specific layout of measuring point in hydroelectric turbine.

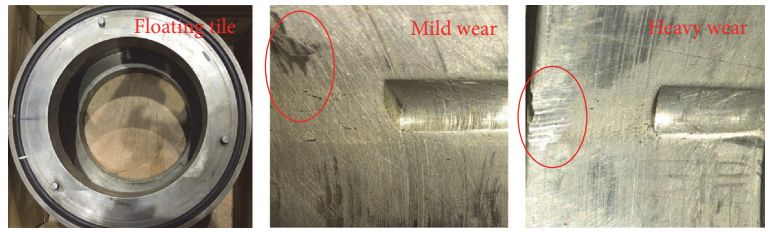

Figure 12: Different conditions of floating tile.

are measured before the turbine blade under mild wear and heavy wear of floating tile, respectively, as shown in Figure 12. Each sampling length is 4000, and the sampling frequency is 227 Hz.

4.2. Fault Diagnosis Result with the Proposed Method. The waveforms and their spectra of the pressure fluctuation signal measured before the turbine blade under two modes of faults in the floating tile are shown in Figures 13(a), 13(b), 14(a), and 14(b), respectively. The fault characteristics frequency of floating tile is 8.95 Hz based on the 5 times of rotating frequency 1.79 Hz, which is aroused by the impact of water on the 5 blades. Due to the high sediment concentration of the Yellow River, the pressure fluctuation signals suffer from serious disturbance during the signal collection and the fault feature of the floating tile is buried in the heavy impulse noise background, while it cannot be clearly identified from time-domain waveform and frequency spectrum. Figures 13(c) and 14(c) show the PE values of the pressure fluctuation signals collected under two modes of faults in the floating tile. Since most of the PE values are larger than 0.9, the experiment pressure fluctuation signals are composed by larger size noise. Take the signals measured before the turbine blade under mild wear of floating tile as an example, and it can be easily seen from that that the PE values have a decrease in a portion of the signals almost from 900 points to 1900 points (highlight in red box of Figure 13(c)), which means there exist some regular sequences in the pressure fluctuation signals.

Based on the variation curves of PE of experiment signals, the signals of which the PE values decrease are selected as the input of Duffing oscillator system to extract the fault feature. Figures 15(a), 15(b), 17(a), and 17(b) display the time-domain waveforms and frequency spectra of the selected signals under two modes of faults in the floating tile. For a large amount of noise is filtered out by PE index, the signal size is reduced from 4000 to 1000, and noise intensity is significantly decreased, which are conducive to identify the fault characteristic frequency. Additionally, the signal component with frequency $f_0 = 8.95$ Hz can be observed from the frequency spectra of the selected signals in Figures 15(b) and 17(b), which is equal to the fault characteristic frequency of floating tile. However, the spectral peak frequency is not prominent and the fault feature cannot be recognized obviously.

Then, according to the regulation of system parameters, a reasonable match between the selected signals and Duffing oscillator model is realized to produce a SR phenomenon with the amplitude-transformation and scale-transformation [40]. As shown in (2), there is a negative correlation between amplitude-transformation coefficient ε and noise intensity D when other parameters remain constant [21]. Thus, the amplitude-transformation and scale-transformation coefficients are set to $\varepsilon = 1/10$ and $R = 100$, and the noise intensity

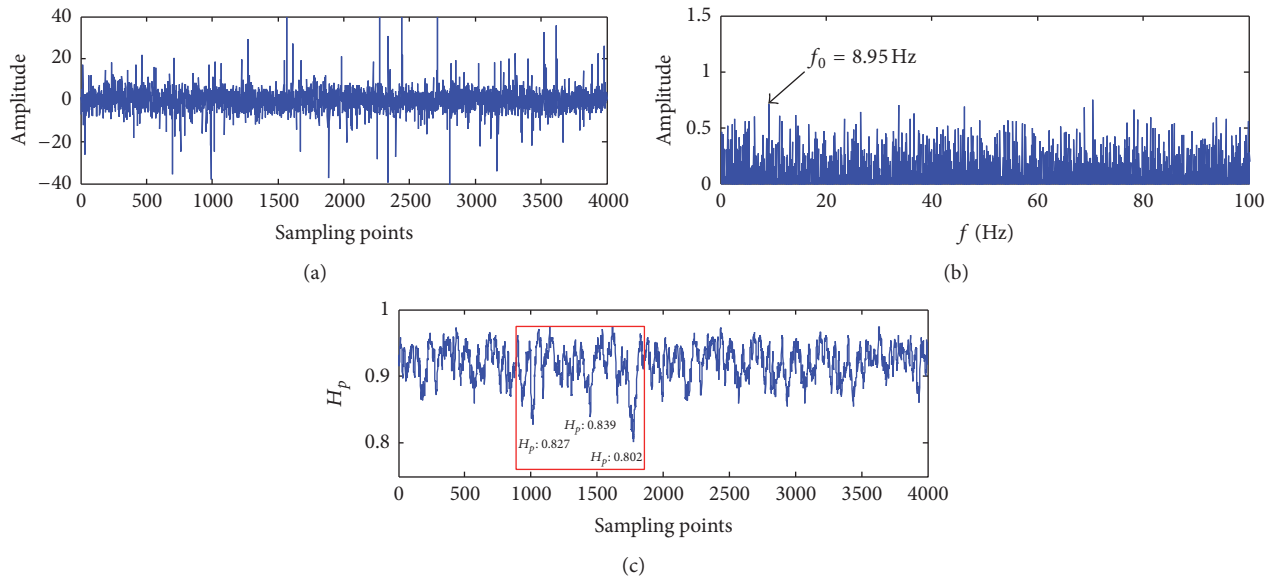

Figure 13: Mild wear of floating tile. (a) Time-domain waveform of original signals, (b) frequency spectrum of original signals, and (c) PE of original signals.

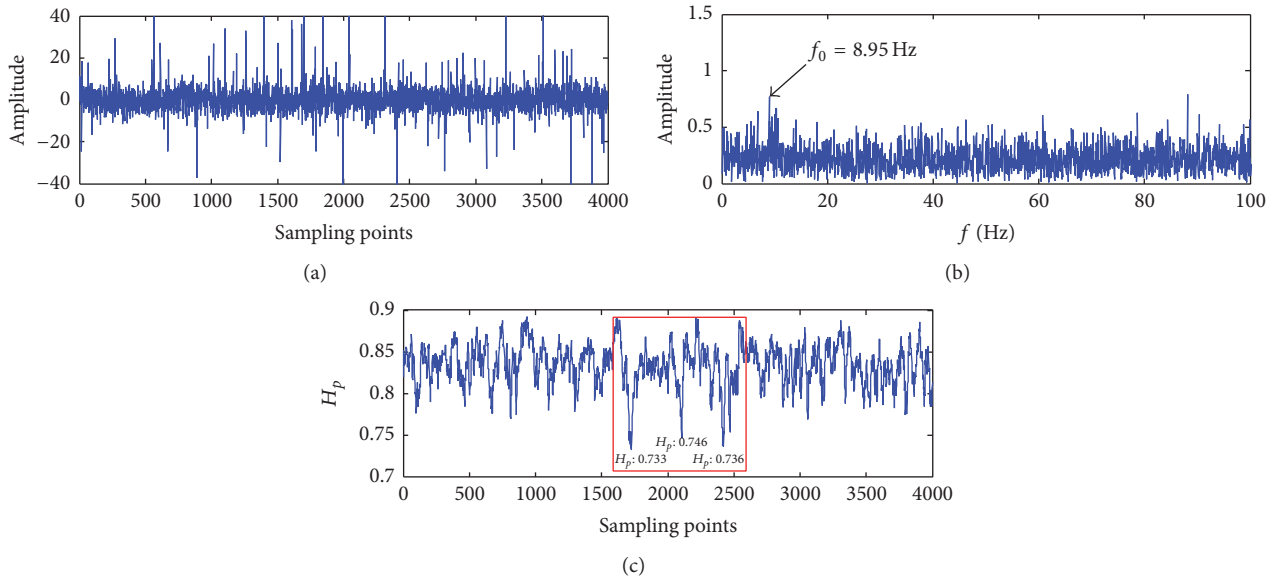

Figure 14: Heavy wear of floating tile. (a) Time-domain waveform of original signals, (b) frequency spectrum of original signals, and (c) PE of original signals.

and signal amplitude of characteristic frequency both have a decrease with the introduction of lower amplitude-transformation coefficient ε. The fault diagnosis results of the proposed method in mild wear and heavy wear of floating tile are illustrated in Figures 15(c), 15(d), 17(c), and 17(d), respectively. Because of the occurrence of SR phenomenon, the energy randomly distributed in the noise has been reduced heavily based on a certain fraction of the noise energy transfers from noise to fault characteristic signal in Duffing oscillator SR system. From the comparison illustrated in Figures 13 and 14, the significant enhancement in the signal amplitude of characteristic frequency $f_0 = 8.95$ Hz is sufficient to provide a means of detecting the fault in the floating tile.

In addition, to validate the feasibility of the proposed method, the fault diagnosis results under two modes of faults in the floating tile with the traditional Duffing oscillator SR method are illustrated in Figures 16 and 18. In order to realize optimal detection result, the amplitude-transformation and scale-transformation coefficients are set to $\varepsilon = 1/10$ and $R = 100$, respectively. Evidently, apart from the fault feature frequency $f_0 = 8.95$ Hz, the frequency spectra in Figures 16(b) and 18(b) contain many complex ingredients, which

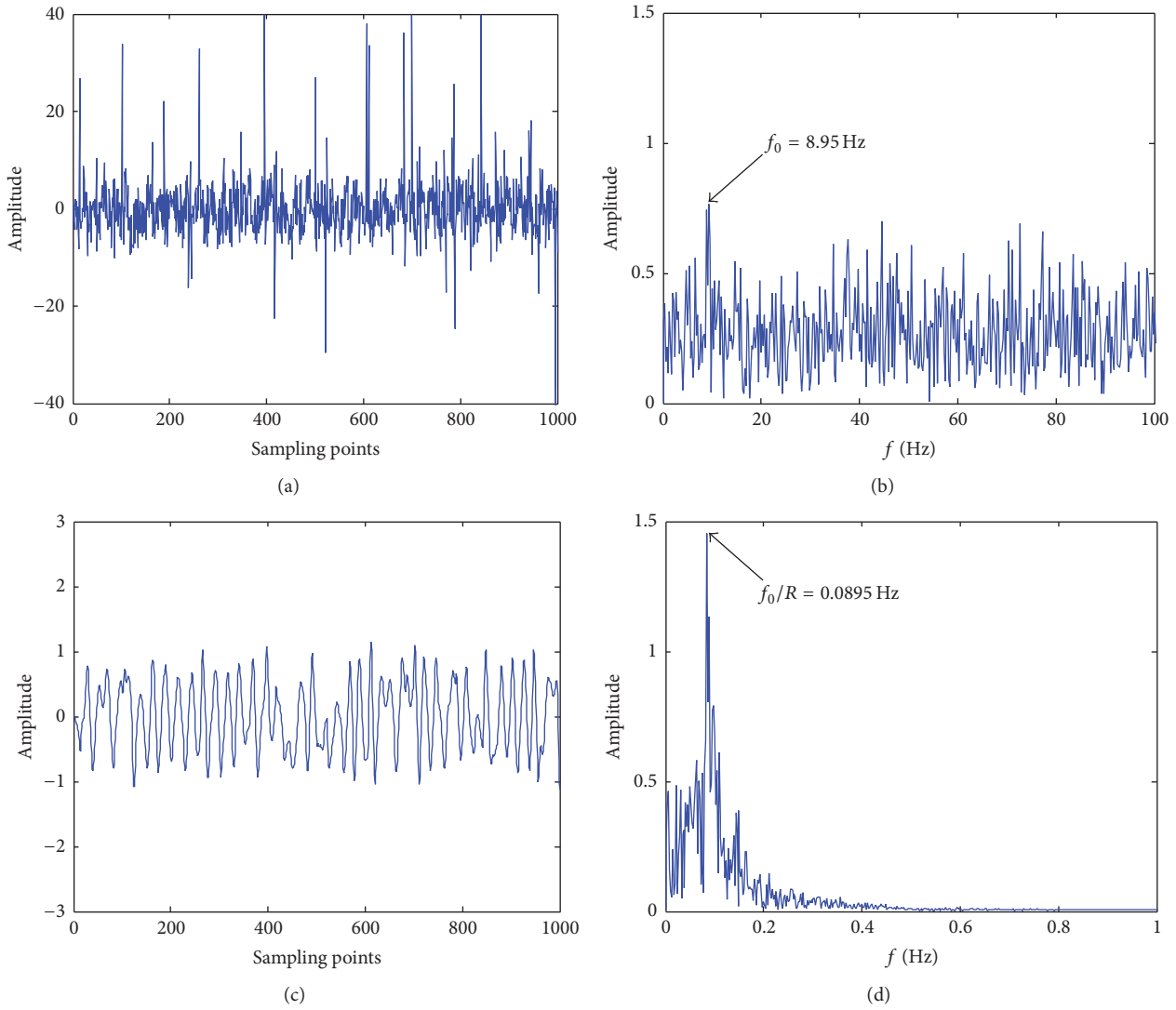

Figure 15: Fault diagnosis result with the proposed method in mild wear of floating tile. (a) Time-domain waveform of selected signals, (b) frequency spectrum of selected signals, (c) time-domain waveform of output signals, and (d) frequency spectrum of output signals. The system parameters are set to $\varepsilon = 1/10$, $R = 100$, $a = 0.3$, $b = 2.2$, and $k = 0.22$.

implies that it is not clear to detect slight fault characteristic signal with the traditional Duffing oscillator SR method.

What is more, due to the larger noise intensity in the input signal of Duffing oscillator system, signal amplitude of characteristic frequency has an obvious decrease, even though the optimal system parameters have been achieved. By contrast, the proposed partly Duffing oscillator SR method has a better effect on the detection of the weak signal of early failure of mechanical system. Therefore, based on the experimental results and above analysis, the proposed partly Duffing oscillator SR method could effectively detect the slight fault feature signals and realize the fault diagnosis of rotating machinery.

5. Conclusion

Due to the fact that the weak signal detecting result of traditional SR method is limited by the noise intensity, a partly Duffing oscillator SR method is proposed to extract the slight fault feature of rotating machinery. In this method, with the induction of PE, the detection of abrupt dynamic change caused by early failure is realized to decrease the signal size and noise intensity and locate the appearance of fault feature, which overcomes the shortcoming of the detecting results limited by noise intensity in traditional SR methods. The collected signals are selected by the variation trend of PE for the input of Duffing oscillator system. Then, according to the regulation of system parameters, a reasonable match between the select signals and Duffing oscillator model is achieved to produce a SR phenomenon to realize the fault diagnosis of rotating machine. The performance of proposed method has been evaluated in the two modes of fault of the hydroelectric turbine in upper reaches of Yellow River. Experiments results verified the effectiveness of the proposed method in weak fault feature extraction and fault diagnosis of the rotating machinery.

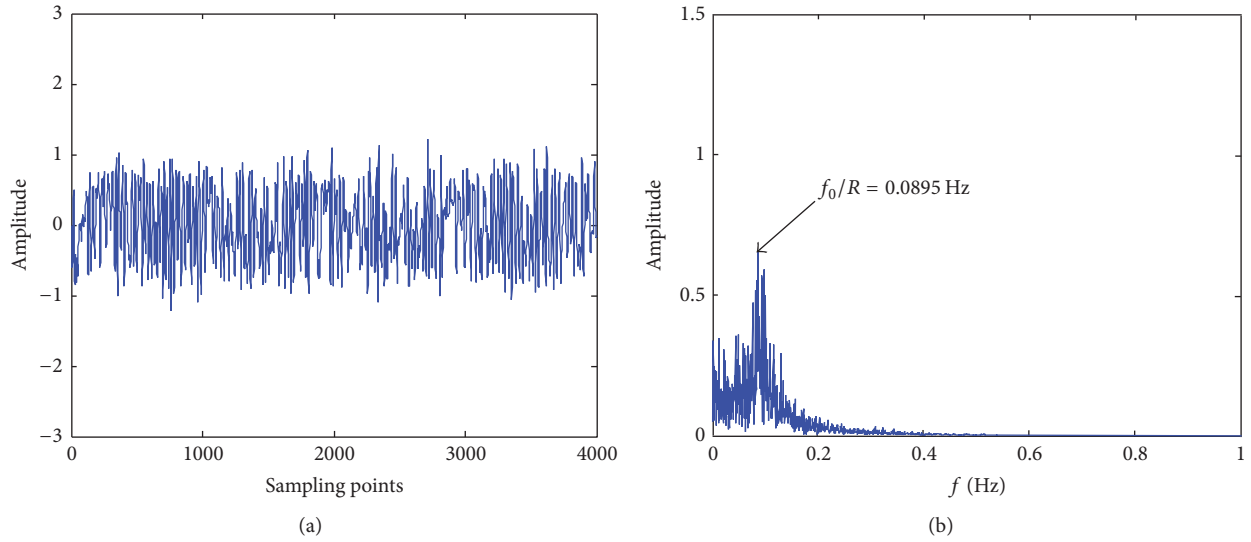

FIGURE 16: Fault diagnosis result with the traditional Duffing oscillator SR method in the mild wear of floating tile. (a) Time-domain waveform of output signals; (b) frequency spectrum of output signals. The system parameters are set to $\varepsilon = 1/10$, $R = 100$, $a = 0.45$, $b = 2.5$, and $k = 0.35$.

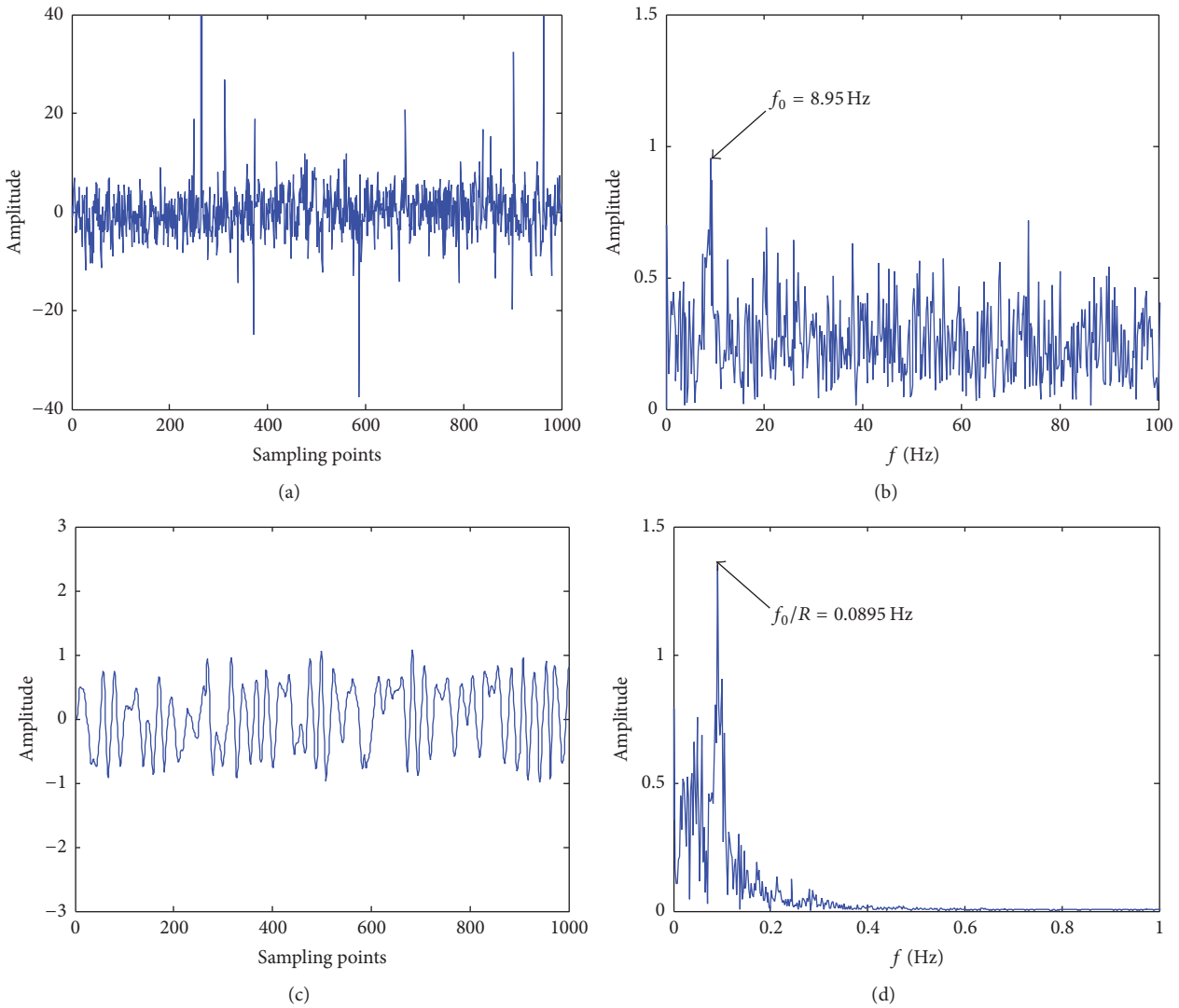

FIGURE 17: Fault diagnosis result with the proposed method in heavy wear of floating tile. (a) Time-domain waveform of selected signals, (b) frequency spectrum of selected signals, (c) time-domain waveform of output signals, and (d) frequency spectrum of output signals. The system parameters are set to $\varepsilon = 1/10$, $R = 100$, $a = 0.31$, $b = 2.1$, and $k = 0.27$.

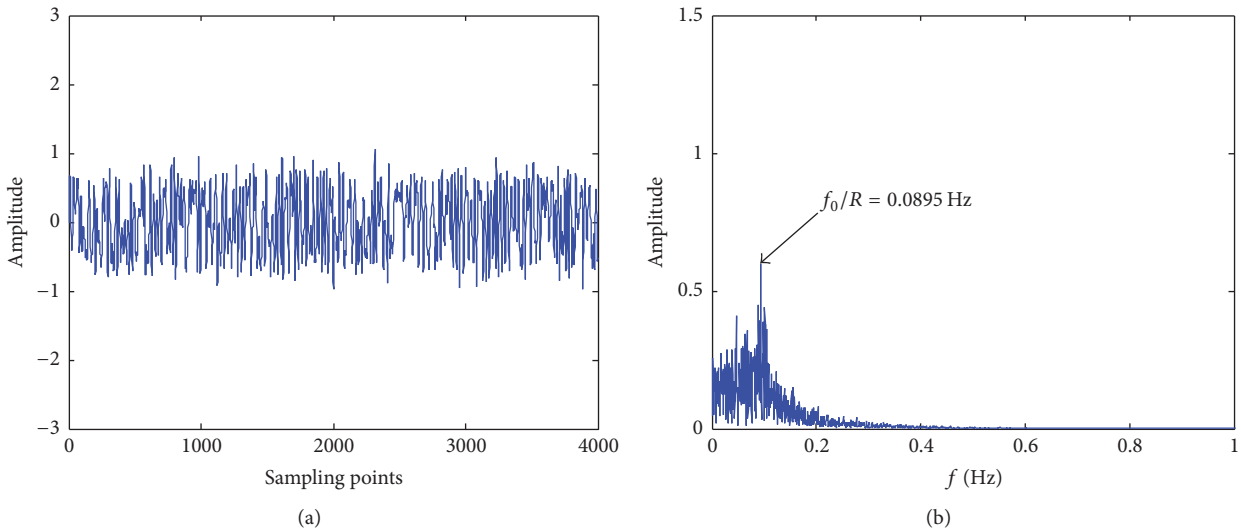

FIGURE 18: Fault diagnosis result with the traditional Duffing oscillator SR method in the heavy wear of floating tile. (a) Time-domain waveform of output signals; (b) frequency spectrum of output signals. The system parameters are set to $\varepsilon = 1/10$, $R = 100$, $a = 0.62$, $b = 3.3$, and $k = 0.32$.

Competing Interests

The authors declare that there are no competing interests regarding the publication of this paper.

Acknowledgments

This research is supported by Key Program of the National Natural Science Foundation of China (Grant no. 51339005), National Natural Science Foundation of China (Grant no. 51279161), and Hydraulic Science and Technology Program of Shaanxi Province (Grant no. 2015slkj-04).

References

[1] D. E. Bently and C. T. Hatch, *Fundamentals of Rotating Machinery Diagnostics*, American Society of Mechanical Engineers, 2002.

[2] Q. Hu, Z. He, Z. Zhang, and Y. Zi, "Fault diagnosis of rotating machinery based on improved wavelet package transform and SVMs ensemble," *Mechanical Systems and Signal Processing*, vol. 21, no. 2, pp. 688–705, 2007.

[3] J. Cheng, D. Yu, J. Tang, and Y. Yang, "Application of SVM and SVD technique based on EMD to the fault diagnosis of the rotating machinery," *Shock and Vibration*, vol. 16, no. 1, pp. 89–98, 2009.

[4] A. D. Nembhard, J. K. Sinha, and A. Yunusa-Kaltungo, "Development of a generic rotating machinery fault diagnosis approach insensitive to machine speed and support type," *Journal of Sound and Vibration*, vol. 337, pp. 321–341, 2015.

[5] J. Chen, Z. Li, J. Pan et al., "Wavelet transform based on inner product in fault diagnosis of rotating machinery: a review," *Mechanical Systems and Signal Processing*, vol. 70, pp. 1–35, 2016.

[6] P. Shi, C. Su, and D. Han, "Fault diagnosis of rotating machinery based on adaptive stochastic resonance and AMD-EEMD," *Shock and Vibration*, vol. 2016, Article ID 9278581, 11 pages, 2016.

[7] R. Benzi, A. Sutera, and A. Vulpiani, "The mechanism of stochastic resonance," *Journal of Physics A*, vol. 14, no. 11, pp. L453–L457, 1981.

[8] C. Nicolis and G. Nicolis, "Stochastic aspects of climatic transitions—additive fluctuations," *Tellus*, vol. 33, no. 3, pp. 225–234, 1981.

[9] V. N. Hari, G. V. Anand, A. B. Premkumar, and A. S. Madhukumar, "Design and performance analysis of a signal detector based on suprathreshold stochastic resonance," *Signal Processing*, vol. 92, no. 7, pp. 1745–1757, 2012.

[10] X.-J. Dong and A.-J. Yan, "Stochastic resonance in a linear static system driven by correlated multiplicative and additive noises," *Applied Mathematical Modelling*, vol. 38, no. 11-12, pp. 2915–2921, 2014.

[11] J. Li, X. Chen, and Z. He, "Multi-stable stochastic resonance and its application research on mechanical fault diagnosis," *Journal of Sound and Vibration*, vol. 332, no. 22, pp. 5999–6015, 2013.

[12] Y. Lei, D. Han, J. Lin, and Z. He, "Planetary gearbox fault diagnosis using an adaptive stochastic resonance method," *Mechanical Systems and Signal Processing*, vol. 38, no. 1, pp. 113–124, 2013.

[13] P. Shi, X. Ding, and D. Han, "Study on multi-frequency weak signal detection method based on stochastic resonance tuning by multi-scale noise," *Measurement*, vol. 47, no. 1, pp. 540–546, 2014.

[14] B. Hu and B. Li, "Blade crack detection of centrifugal fan using adaptive stochastic resonance," *Shock and Vibration*, vol. 2015, Article ID 954932, 12 pages, 2015.

[15] J. Li, X. Chen, Z. Du, Z. Fang, and Z. He, "A new noise-controlled second-order enhanced stochastic resonance method with its application in wind turbine drivetrain fault diagnosis," *Renewable Energy*, vol. 60, pp. 7–19, 2013.

[16] L. Gammaitoni, F. Marchesoni, E. Menichella-Saetta, and S. Santucci, "Stochastic resonance in bistable systems," *Physical Review Letters*, vol. 62, no. 4, pp. 349–352, 1989.

[17] L. Gammaitoni, E. Menichella-Saetta, S. Santucci, F. Marchesoni, and C. Presilla, "Periodically time-modulated bistable systems: stochastic resonance," *Physical Review A*, vol. 40, no. 4, pp. 2114–2119, 1989.

[18] P. Jung and P. Hanggi, "Resonantly driven Brownian motion: basic concepts and exact results," *Physical Review A*, vol. 41, no. 6, pp. 2977–2988, 1990.

[19] W. Fu-Zhong, C. Wei-Shi, Q. Guang-Rong et al., "Experimental analysis of stochastic resonance in a Duffing system," *Chinese Physics Letters*, vol. 20, no. 1, p. 228, 2003.

[20] Y.-G. Leng, Z.-H. Lai, S.-B. Fan, and Y.-J. Gao, "Large parameter stochastic resonance of two-dimensional Duffing oscillator and its application on weak signal detection," *Acta Physica Sinica*, vol. 61, no. 23, Article ID 230502, 2012.

[21] Z.-H. Lai and Y.-G. Leng, "Generalized parameter-adjusted stochastic resonance of duffing oscillator and its application to weak-signal detection," *Sensors (Switzerland)*, vol. 15, no. 9, pp. 21327–21349, 2015.

[22] M. Zanin, L. Zunino, O. A. Rosso, and D. Papo, "Permutation entropy and its main biomedical and econophysics applications: a review," *Entropy*, vol. 14, no. 8, pp. 1553–1577, 2012.

[23] R. Yan, Y. Liu, and R. X. Gao, "Permutation entropy: a nonlinear statistical measure for status characterization of rotary machines," *Mechanical Systems and Signal Processing*, vol. 29, pp. 474–484, 2012.

[24] D. Han, S. An, and P. Shi, "Multi-frequency weak signal detection based on wavelet transform and parameter compensation band-pass multi-stable stochastic resonance," *Mechanical Systems and Signal Processing*, vol. 70, pp. 995–1010, 2016.

[25] L. Alfonsi, L. Gammaitoni, S. Santucci, and A. R. Bulsara, "Intrawell stochastic resonance versus interwell stochastic resonance in underdamped bistable systems," *Physical Review E*, vol. 62, no. 1, pp. 299–302, 2000.

[26] L. Gammaitoni, P. Hänggi, P. Jung, and F. Marchesoni, "Stochastic resonance," *Reviews of Modern Physics*, vol. 70, no. 1, pp. 223–287, 1998.

[27] J. Harmouche, C. Delpha, and D. Diallo, "Incipient fault detection and diagnosis based on Kullback-Leibler divergence using Principal Component Analysis—part I," *Signal Processing*, vol. 94, no. 1, pp. 278–287, 2014.

[28] G. Yang, Y. Liu, Y. Wang, and Z. Zhu, "EMD interval thresholding denoising based on similarity measure to select relevant modes," *Signal Processing*, vol. 109, pp. 95–109, 2015.

[29] A. Komaty, A. Boudraa, and D. Dare, "EMD-based filtering using the Hausdorff distance," in *Proceedings of the IEEE International Symposium on Signal Processing and Information Technology (ISSPIT '12)*, pp. 292–297, December 2012.

[30] R. Yan and R. X. Gao, "Approximate Entropy as a diagnostic tool for machine health monitoring," *Mechanical Systems and Signal Processing*, vol. 21, no. 2, pp. 824–839, 2007.

[31] A. Lempel and J. Ziv, "On the complexity of finite sequences," *IEEE Transactions on Information Theory*, vol. 22, no. 1, pp. 75–81, 1976.

[32] S. M. Pincus, "Approximate entropy as a measure of system complexity," *Proceedings of the National Academy of Sciences of the United States of America*, vol. 88, no. 6, pp. 2297–2301, 1991.

[33] C. Bandt and B. Pompe, "Permutation entropy: a natural complexity measure for time series," *Physical Review Letters*, vol. 88, no. 17, pp. 1741021–1741024, 2002.

[34] B. Fadlallah, B. Chen, A. Keil, and J. Príncipe, "Weighted-permutation entropy: a complexity measure for time series incorporating amplitude information," *Physical Review E*, vol. 87, no. 2, Article ID 022911, 2013.

[35] Y. Cao, W. Tung, J. B. Gao, V. A. Protopopescu, and L. M. Hively, "Detecting dynamical changes in time series using the permutation entropy," *Physical Review E. Statistical, Nonlinear, and Soft Matter Physics*, vol. 70, no. 4, Article ID 046217, 2004.

[36] K. Keller and M. Sinn, "Ordinal analysis of time series," *Physica A: Statistical Mechanics and Its Applications*, vol. 356, no. 1, pp. 114–120, 2005.

[37] N. Nicolaou and J. Georgiou, "Detection of epileptic electroencephalogram based on permutation entropy and support vector machines," *Expert Systems with Applications*, vol. 39, no. 1, pp. 202–209, 2012.

[38] F. C. Morabito, D. Labate, F. La Foresta, A. Bramanti, G. Morabito, and I. Palamara, "Multivariate multi-scale permutation entropy for complexity analysis of Alzheimer's disease EEG," *Entropy*, vol. 14, no. 7, pp. 1186–1202, 2012.

[39] M. Staniek and K. Lehnertz, "Parameter selection for permutation entropy measurements," *International Journal of Bifurcation and Chaos*, vol. 17, no. 10, pp. 3729–3733, 2007.

[40] J. Tan, X. Chen, J. Wang et al., "Study of frequency-shifted and re-scaling stochastic resonance and its application to fault diagnosis," *Mechanical Systems and Signal Processing*, vol. 23, no. 3, pp. 811–822, 2009.